Evaluation of the shape of the specular peak for high glossy surfaces

Gaël Obein*, Shiraz Ouarets, Guillaume Ged

Laboratoire Commun de Métrologie LNE-CNAM
61 rue du Landy, 93210 La Plaine St Denis
France

ABSTRACT

Gloss is the second most relevant visual attribute of a surface beside its colour. While the colour originates from the wavelength repartition of the reflected light, gloss originates from its angular distribution. When an observer is asked to evaluate the gloss of a surface, he always first orientate his eyes along the specular direction before lightly tilting the examined sample. This means that gloss is located in and around the specular direction, in a peak that is called the specular peak. On the one hand, this peak is flat and broad on matte surfaces on the other hand, it is narrow and sharp on high gloss surfaces. For the late ones, the FWHM of the specular peak is less than 2° which can be quite difficult to measure. We developed a dedicated facility capable of measuring specular peak with a FWHM up to 0,1 °. We measured the evolution of the peak according to the angle of illumination and the specular gloss of the sample in the restricted field of very glossy surface. The facility and peaks measured are presented in the paper. The next step will be to identify the correlations between the peak and the roughness of the sample.

.

Keywords: Gloss, BRDF, metrology, specular peak, material, appearance.

1. INTRODUCTION

Objects that have identical shapes can be identified through their visual surface attributes, which are colour, texture, gloss, transparency, opacity, etc.. The compilation of these visual attributes gives the appearance of the surface [1].

Amongst this list of attributes of the visual appearance, gloss is known to be the second most relevant beside color [2][3]. From a purely qualitative point of view, gloss is related to both sensations of sturdiness and quality. For this reason, its control and mastery is crucial for diverse industries, for instance automotive, cosmetics, paper, printing, packaging, coatings, plastics, food, etc., because it is directly implicated in the customer satisfaction. However, gloss is more than an "aesthetic" attribute and might play a more important role than we think in the global perception of our environment. Gloss helps in the perception of the curvature of the surface, in the recognition of the nature of the material, or in the process of color constancy. This list may yet be just at its beginning as the interest of the scientific community on the role played by gloss in visual perception is recent.

As a matter of fact, in the vision community, the XXth century has been devoted to the study, the comprehension and the measurement of color. Colorimetry is now an advanced science and progresses on sound basis. On the other side, very few efforts have been done on gloss perception and comprehension-save for high gloss levels, where the automotive industry has done a good job. For the past ten years though, things have been changing. From a fundamental point of view, the role of gloss in the total perception is now obvious. From an applied point of view as well, the industrial needs have recently evolved. Midglossy car paintings appeared, 2.5D printers rise gloss issues, deep mat finish are requested for laptop computers or smartphones, etc…

In order to maintain a good level of quality, and to generate innovation in the interesting field of glossy aesthetic effect, the industry needs a good metrology. Unfortunately, the field of gloss metrology is still quite poor regarding to what is available for the color. The most popular measurement is the specular gloss, which compares flux reflected in the specular direction, in a given solid angle by the sample and the flux reflected by a standard, which is a surface perfectly polished of given refractive index [4]. This measurement gives a good correlation with the visual sensation at a first order [5][6]. It is fast and useful to evaluate relative variations of gloss for a given production and in a given environment. However, the specular gloss is a bad absolute gloss measurement. It varies drastically with the direction of

*gael.obein@cnam.fr; phone +33 158 808 788.

illumination or with the diffuse component of the illuminant where the sensation of gloss undergoes only small variations [5][7][8][9].

Other possibilities of measurements are proposed today and give promising perspectives, based on more sophisticated optical designs (see for example the EZ-Contrast® from Eldim or the Rhopoint-IQ® from Rhopoint Instrument). If these new instruments are able to carry on a better analyze of the light reflected by the sample, the relation between the values they provide and the sensation of gloss is still blur and not well understood.

From a perceptive point of view, we know that sensation of gloss doesn't only come from the luminous flux reflected in the specular direction. For instance, Vienot & Obein compared the gloss of piece of tire tube and of a black inked paper [10]. Even if both samples reflected almost the same luminous and have almost the same specular gloss value, the difference of visual gloss was obvious and all the observers where able not only to graduate the gloss, but also the retrieve the material of which the sample was made of.

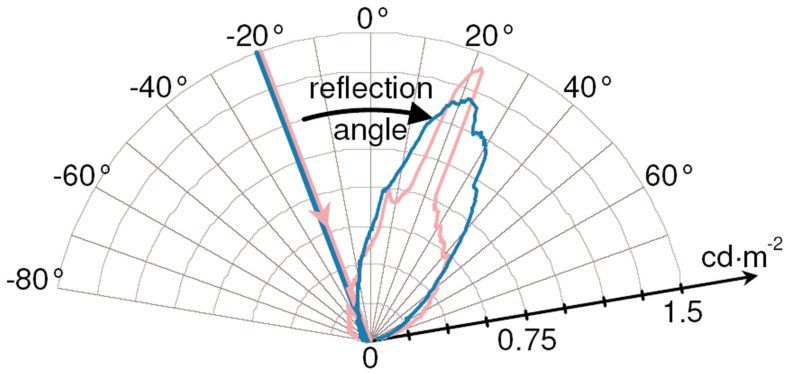


Figure 1: Section of the specular peak in the plane of incidence, for a piece of black rubber (pink curve) and the sample N009® of the 3C gloss scale made of coated cardboard (specular gloss 60 ° = 4,9 gu) (blue curve). Incident angle of 20 ° from the normal (from [10]. The observers are able to extract the information on the gloss and on the material from the shape of the specular peak.

A study of the angular repartition of the reflected light revealed that the shape of the specular peak was very different between the two samples and suggested that the visual system extracts information not only from the size of the peak, but also from the shape of the peak (figure 1).

Ged et al confirmed this hypothesis in a more complete study on black gloss scale made of different type of materials and different type of roughness [11]. If they have been able to separate different components of gloss from a visual data, the physical origin of these components was difficult to analyze accurately, mainly because the angular resolution of 0,5 ° of their instrument was too low. It seems that the observers were able to find indices in the specular peak with a better resolution. Other recent studies reveals that the observers are able to find more information than only the gloss in the specular peaks suggesting that they process the shape of specular peak with a very high attention [12]. This assumption is confirmed at a very intuitive level when we give a sample to an observer and question him on the gloss of the object. The observer systematically search for the specular direction and then moves its look around the specular, suggesting an attentive scan of the angular repartition of the light around the specular, and thus a fine evaluation of the shape of the specular peak.

From an instrumental point of view, the devices proposing a way to measure the shape of a specular peak with a very high angular resolution are unfortunately rare. The reason for this lack is very pragmatic. First, would you want a high angular discrimination, you would have to decrease the solid angle of observation -and thus reach very low flux levels. Then, you should perform very little angular displacements between each measurement, which implies a drastic increase in measurements duration.

In this paper, we describe our new set-up developed at LNE-CNAM, the national metrological institute for France. This device was built to perform specular peak measurements with an angular resolution better than the one of the human eye. The device is thus able to acquire at least the same level of information present in the specular peak than the human visual system. We hope that this metrological facility will provide new keys for the study and the understanding of gloss perception, and gloss metrology.

2. DESCRIPTION OF THE EQUIPMENT

This set up devoted to the specular peak measurement shares a mechanical part common with our gonioreflectometer devoted to absolute measurement of BRDF. A general view of the facility is proposed on figure 2 [14]. For the spatial line, our objective was to reach an angular resolution at least equal to the angular resolution of the human eye which is assumed to be 2' for a normal vision. It means that we have to target an angular resolution of at least 0,03°.

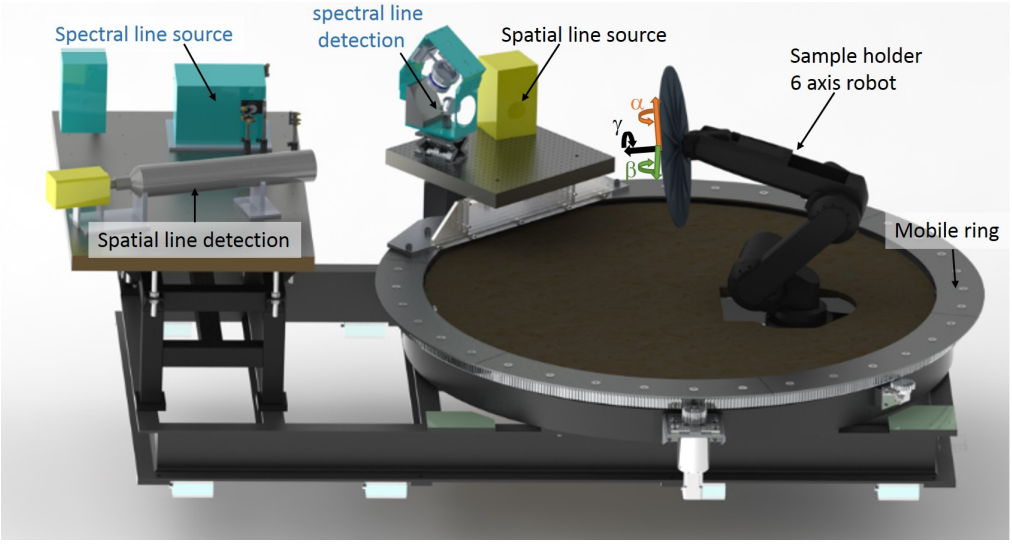


Figure 2: General view of the facility. One line is devoted to absolute BRDF measurement, with a static monochromatic illumination and a mobile broadband detection (280 – 900 nm). One line is devoted to the specular peak measurement with a mobile broadband illumination (QTH) and a static Fourier transform base detection. The sample holder and the ring for the rotation around the sample is shared between the 2 lines.

2.1 Illumination

The illumination part is made of a 200 W QTH lamp, and an optical system that allows to illuminate the sample with a collimated light beam. In order to reach an angular resolution of 0.03 °, this beam's divergence has to be lower than 0.03 °. This is obtained by using a pinhole of 200 µm of diameter and a doublet f=400 mm. A collimator system allows to image the lamp filament on the pinhole. The shape of the beam at the exit of the illumination part is circular and can be adjusted between 1 up to 20 mm of diameter according to the sample under test. For instance, for a small piece of glossy plastic, the diameter will be reduced to avoid vignetting effects at grazing angles. For a piece of textile, the diameter will be large in order to average the effect of the texture of the fibers.

2.2 Sample holder

The sample holder is a 600 mm diameter plate. It allows to carry on measurements at gazing angles (up to 88 °) even with a illumination of 20 mm of diameter. Once more, the dimensions have been chosen in order to carry on measurements on textiles, but we can imagine doing measurements on road coatings or other mat materials.

The plate is mounted at the extremity of a six axes robot arms that can undergo 12 kg. The robot performs three rotations around the axes α, β and γ (see figure 2). The fourth rotation is obtained with the ring bearing the illumination part. The three remaining degrees of freedom are used for a translation along the three axis *x, y* and *z* (see figure 2) that allows to put the surface of the sample at the center of the gonioreflectometer.

Using this system, we are then able to generate all the angular configurations defined by a given direction of illumination and a given direction of observation, belonging to the half sphere above the sample's surface. Measurements in transmission are under study, but will be limited in term of angular configurations range.

2.3 Detection

For the acquisition of the signal reflected by the sample, we used the gonioreflectometer and a detection based on the combination of Fourier optics and a high sensitivity CCD camera [15]. This system has been successfully implemented

for Bidirectionnal Reflectance Factor measurements (BRF, see [16]), by Eldim (see the EZ-Contrast® and related products on http://www.eldim.fr). Our detection was developed in collaboration with Eldim according to the following principles:

The optical system plays the role of a simple lens, and provides a Fourier transform image of the material surface. Every light beam reflected from the test area with, for instance, a $\theta_r = \theta_{R1}$ exiting angle, is focused on the focal plane at the same azimuth and at a position $[x_{r1}, y_{r1}] = F(\theta_{R1}, \varphi_{R1})$. The luminance geometry $L(x_{r1}, y_{r1})$ is quickly recorded through the CCD sensor and easily returns the angular characteristics of the light reflected by the sample.

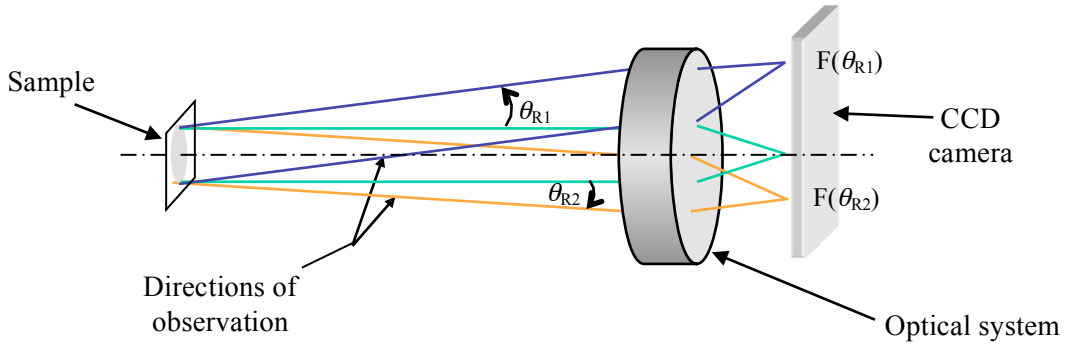


Figure 3: Principle of the detection based on the Fourier optic: All the light reflected in a given direction, defined by its zenith angle θ_R and azimuthal angle φ_R,, is focused in one point at the focal plane of the optical system. The coordinates $[x_R, y_R]$ of the point are related to θ_R and φ_R. The luminance at this point is recorded on a 512 × 512 pixels CCD camera. In one shot, the luminance in more than 200000 directions of reflection can be recorded.

The system looks through a field of ±1° and is located at a distance of 1700 mm from the center of the sample. A first objective made of two lenses converts the beam in the Fourier plane. The first lens of this optical system has a diameter of 110 mm. The Fourier plane is then transported on the CCD camera sensor thanks to second optical system made of two other lenses. A photometric V(λ) filter is used to restrict the spectral domain to the photometry and to provide a measurement proportional to the luminance. The external length of the system is 663 mm.

For the flux measurement, we use a high sensitivity cooled CCD camera (Hamamatsu ORCA II). The sensor is a matrix of 512 by 512 pixels. The size of a pixel is 24 by 24 µm. The combination of both water and Peltier cooling maintains a working temperature of -70 °C. The quantum efficacy of the CCD is optimized for the visible while a 16 bits A/D converter generates a high dynamic range. The mechanical shutter is able to drop at an exposure time of 20 ms.

From the description above, we can say that the ultimate angular resolution of the complete system could be

$$\Delta_{ult} = \frac{\pm 1^\circ}{512 \text{pixels}} = 0{,}004^\circ \qquad (1)$$

Nonetheless, such a resolution can only be achieved with an incident beam collimated better than Δ_{ult}. This observation imposes the use of a pinhole of diameter inferior to 28 µm and hence a reduction of the flux by a factor 50. For this first attempt, we decided to keep some possibility of improvement and used a pinhole of 200µm of diameter. Consequently, the resolution on our present measurements is only limited by the incident beam diameter.

3. PERFORMANCE OF THE EQUIPMENT

3.1 Linearity

In order to improve the dynamic range of the measurement we use a multiple exposure time method. The first exposure time is calculated in order to avoid saturation of the most exposed pixel of the CCD. It gives the picture P1. Then we increase the exposure time by a factor two. It gives the picture P2. Assuming that the shutter is perfectly synchronized and that the pixels filling capacity is linear with the luminous flux, we can divide the number of counts in each pixel of the picture P2 by a factor two and paste the unsaturated pixels of P2 in the picture P1. Doing that, we increase the

number of bit by one unit in the picture, for the dark pixels in picture P1. We can repeat this process with a longer exposure time.

In order to validate that method, the linearity of the camera has been tested in flux and in time (figure 4). All the measurements have been done using a Spectralon® as sample. This sample behaves almost similarly as a perfect diffuser when it is illuminated from a direction perpendicular to its surface, and we you look in a "non-overgrazing" direction. For the measurements, the zenith of illumination was 0°, and the zenith of observation was approximately 10°. Assuming the lambertian behavior of the sample, the value retained for the measurements was the median of the CCD matrix.

The linearity, in terms of flux, is tested using neutral filters in order to change the luminance value without modifying the spectrum (fig4 left). We tested 7 different exposure times (only 6 are reported) and up to 4 levels of luminance. Results show that our camera is quite linear between $2 \cdot 10^3$ and $6 \cdot 10^4$ count. Out of this domain, the values are not linear and have to be removed.

The linearity, in terms of time, is tested by maintaining a constant flux and changing the exposure time t by a factor 2, between t_{min}=0,02s and t_{max}= 80s.

For t_{n-1} we measure the number of count x_{n-1} and with $t_n = 2 \times t_{n-1}$ we measure the number of count x_n. Then we compute the linearity correcting factor $K(n)$

$$\begin{cases} k_n = \dfrac{2x_{n-1}}{x_n} \\ K(n) = \prod_{1}^{n} k_n \end{cases} \tag{2}$$

For an ideal camera, k(n) =1. Our results show that a correction must be applied on the measurements.

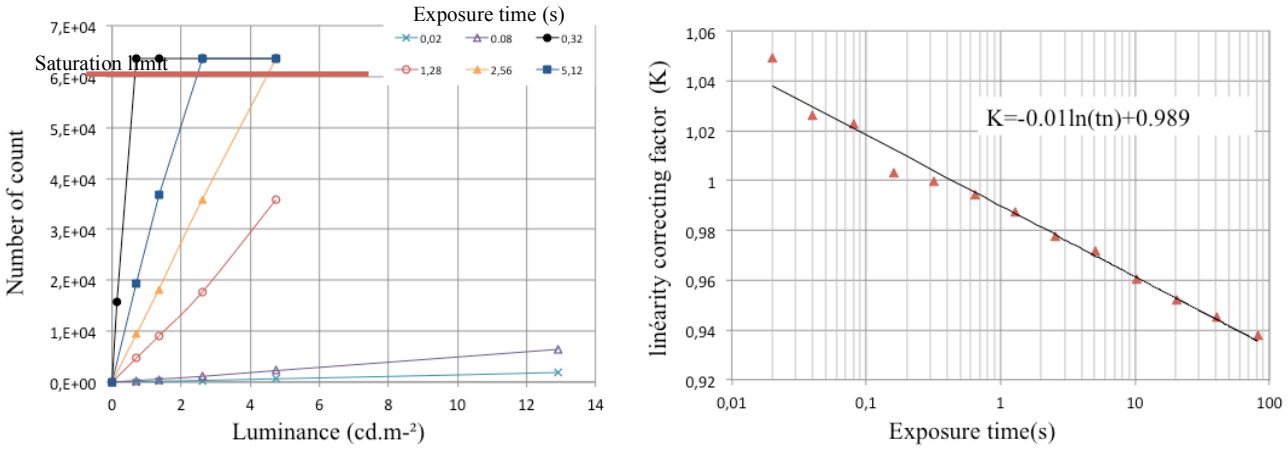


Figure 4: Characterization of the linearity of the camera. Left, linearity in flux. The exposure time is maintained constant and the luminance varies. The number of count on the CCD is recorded. Right, linearity in time. The luminance is constant and the exposure time varies. The linearity factor K is reported and modeled by a root mean square line

3.2 Resolution

The angular resolution of the set-up has been tested using a mirror as sample. As a matter of fact, for a perfect mirror, all the light is reflected in the specular direction. Thus, specular peak for a mirror is a Dirac function and the answer of our device to such a stimulus will give its transfer function. As expected, we measure a specular peak with a full width at half maximum (FWHM) of less than 8 pixels, which gives 0,03°. This peak is due to the divergence of the incident beam (figure 5).

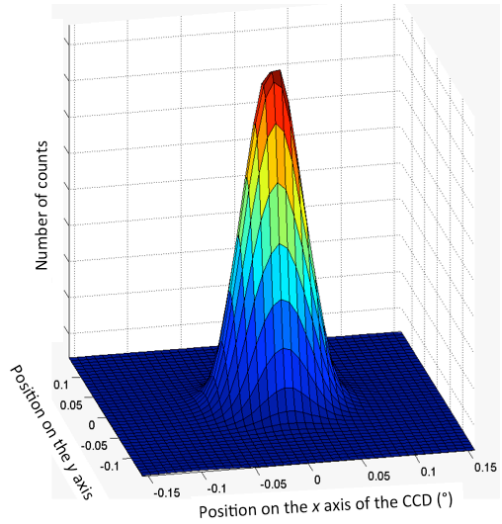


Figure 5 : Transfer function of the detection, obtained using a mirror as sample. The signal is centered on the CCD matrix. The full width at half maximum is less than 8 pixels, which gives an angular resolution better than 0,03°

RESULTS ON A GLOSSY SAMPLE

3.3 Sample

To conclude this work, we decided to perform a measurement on a real glossy sample. We have chosen the black inked paper N001, providing from the 2C - Color & Consulting gloss scale. This sample has a specular gloss value at 60° of 91 (figure 6).



Figure 6 : Sample N001 from the 2C – Color & Consulting gloss scale. Specular gloss at 60° of 91 gu (gloss unit). Color black. Ink on paper.

This sample has already been measured with an EZ-Contrast, at an incidence of 45°. The specular peak had a FWHM = 1,2°, but the resolution was 0,4°. We repeated this measurement in the same configuration with our high-resolution detection.

The direction of illumination **I** is $\theta_I = 45°$ and $\varphi_I = 180°$. ·The foot of the peak will spread on an area larger than ± 1°. In order to have measurement of the full peak, we have to combine the rotations of the gonioreflectometer and the Fourier detection. We did 9 pictures, according to 9 measurements directions defined by their zenithal and azimuthal angles, respectively θ_S and φ_S. These directions are reported in the following table :

Picture #	1	2	3	4	5	6	7	8	9
θ_S	43,5°	45°	46,5°	43,5°	45°	46,5°	43,5°	45°	46,5°
φ_S	1,5°	1,5°	1,5°	0°	0°	0°	-1,5°	-1,5°	-1,5°

3.4 Measurement

Using our detection, we obtain the 9 following pictures on the CCD. Each picture is a compilation of 3 exposure times in order to increase the dynamic range.

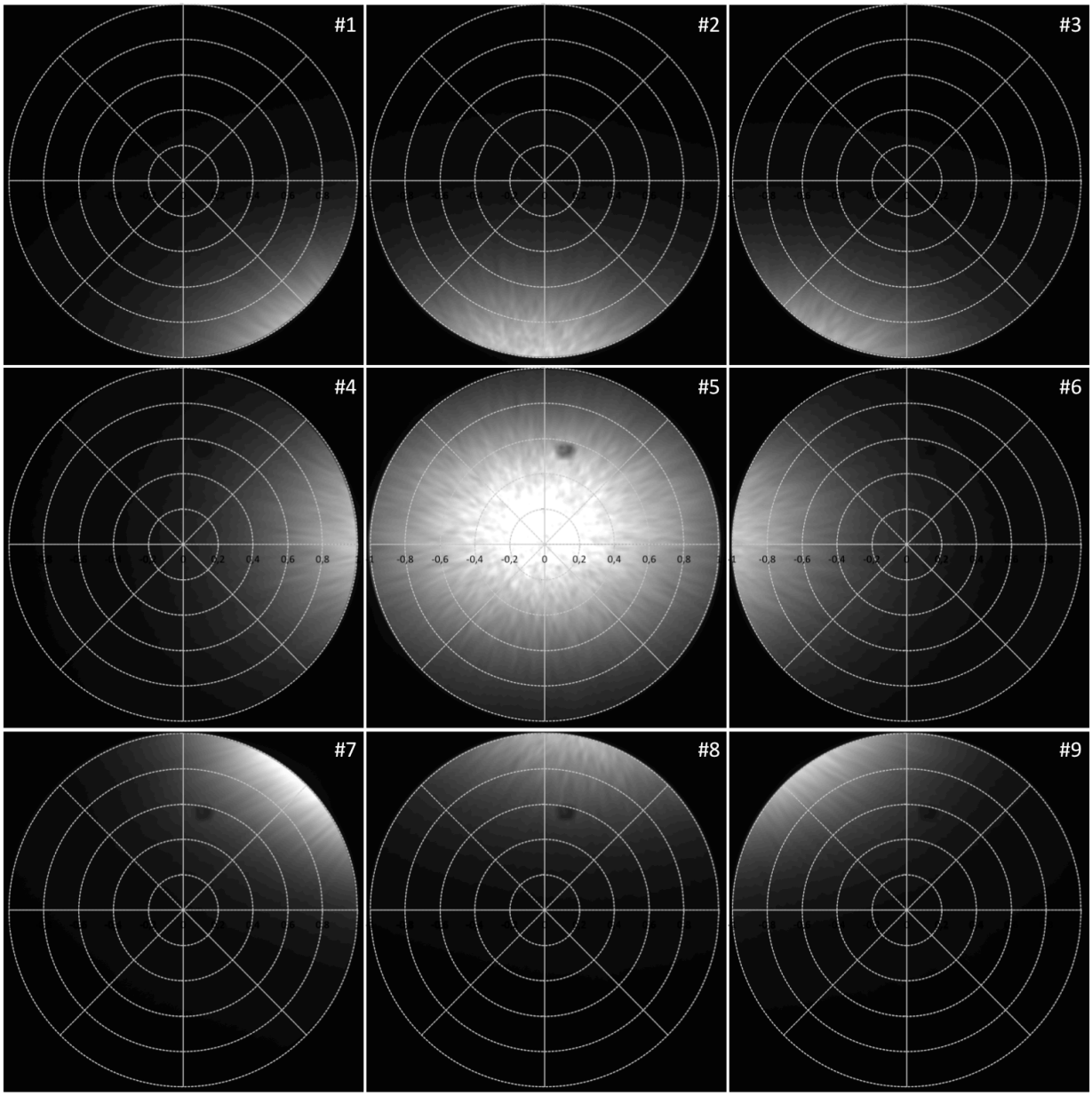


Figure 7: The 9 pictures used for the construction of the specular peak of the sample N001 for an incidence at a zenith 45°. Each picture is centered on a given direction of observation. From the center, the eccentricity is Δθ. The azimuth is Δφ.

3.5 Recombination of the peak

From the 9 pictures above, we have to reconstruct the complete specular peak. From a theoretical approach this operation wass not as simple as it seemeed on the puzzle builder's point of view. As a matter of fact, the luminances captured in the Fourier plane of the detection are relatives to the direction of observation **S** (θ_S ; φ_S) which corresponds to the center of the CCD (x=0, y=0). For instance, the direction **R** corresponding to the pixel (x,y) in the camera can be expressed according to the angles Δθ and Δφ, where Δθ and Δφ are the relative zenithal and azimuthal angles according to the direction **S**. we have

$$\Delta\theta = \sqrt{x^2 + y^2} \quad \text{and} \quad \Delta\varphi = \tan^{-1} y/x \tag{3}$$

However the expression of the absolute zenithal and azimuth angles of the direction **R** (θ_R ; φ_R) according to θ_S , φ_S , $\Delta\theta$ and $\Delta\varphi$ is not trivial and can not be developed in this article. The result is given in the following expression:

$$\mathbf{R} = \left(\cos\Delta\theta + \frac{\cos\Delta\varphi \cdot \sin\Delta\theta}{\tan\delta}\right)\cdot\mathbf{S} - \frac{\cos\Delta\varphi \cdot \sin\Delta\theta}{\sin\delta}\cdot\mathbf{I} + \frac{\sin\Delta\varphi \cdot \sin\Delta\theta}{\sin\delta}\cdot(\mathbf{I}\wedge\mathbf{S}) \tag{4}$$

Where,

- **I**, **S** and **R** are unit vectors starting from the center of the sample and pointing respectively the direction of illumination **I** (θ_I ; φ_I), the direction of observation of the center of the detection **S** (θ_S ; φ_S) and the direction of observation corresponding to the pixel (x,y), **R**(θ_R ; φ_R)
- $\Delta\theta$ and $\Delta\varphi$ are the relative zenithal and azimuthal angles according to the direction **S**
- δ is the angle between **I** and **S**.

$$\delta = \cos^{-1}\left(\sin\theta_{\mathbf{I}}\sin\theta_{\mathbf{R}}\cos(\varphi_{\mathbf{R}} - \varphi_{\mathbf{I}}) + \cos\theta_{\mathbf{I}}\cos\theta_{\mathbf{R}}\right) \tag{5}$$

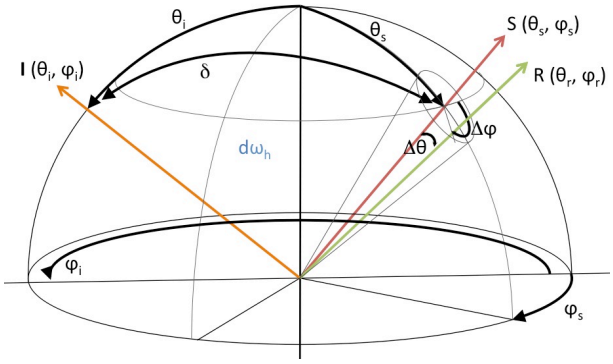


Figure 8 : Representation of the different unit vectors :
I (θ_I ; φ_I), the direction illumination
S (θ_S ; φ_S), the direction of the center of the detection
R (θ_r ; φ_r), the direction of observation

3.6 Result

It is therefore possible to calculate, for each pixel of each of the 9 pictures, the polar coordinates (θ_R ; φ_R) of the corresponding vector **R**. We end with a full matrix, containing the information on the luminance reflected by the sample for a zenithal angle $42{,}5° < \theta_R < 47{,}5°$ and an azimuthal angle $-2{,}2° < \varphi_R < 2{,}2°$ with a step $\delta\theta = \delta\varphi = 2/521 = 0{,}004°$. The number total of direction of observation reported is thus about 1,4M… A graph of the peak is proposed in figure 9.

4. CONCLUSION

Gloss is a visual attribute of surfaces that plays an important role in the visual perception. From an industrial point of view, gloss is associated with quality and has an important part to the aesthetical aspect of a material. It is therefore essential to control it. Whatever its importance, gloss cannot be reduced to mere aestheticism. Recent studies showed that our visual system constructs the coherence of the scene surrounding us by using the gloss of the different material. The shape of the surfaces, the spectrum and the position of the illuminant are partially deducted from the gloss. Such results are exciting. From a metrological point of view, gloss is a young quantity which needs more attention from the metrologist, and more sophisticated equipment than the well-tried though dated glossmeters or hazemeters. At LNE-CNAM, we developed in collaboration with Eldim company, a new facility devoted to the measurement and the study of gloss. This equipment performs measurements of the luminance reflected by the sample in the specular region, where the information on the gloss is located. The direction of illumination can be chosen everywhere in the half-space and the size of the incident beam can go up to 20mm of diameter, with a QTH spectrum (color temperature adjustable). The sample measured can be large and not necessary flat or rigid. A dedicated detection has been developed. The principle is based on the optical Fourier transform and allows to measure in few seconds the luminance reflected in a cone of plus or minus 1°, with a theoretical angular discrimination of 0,004°. But to reach such a performance, the incident beam need to be collimated better than that.

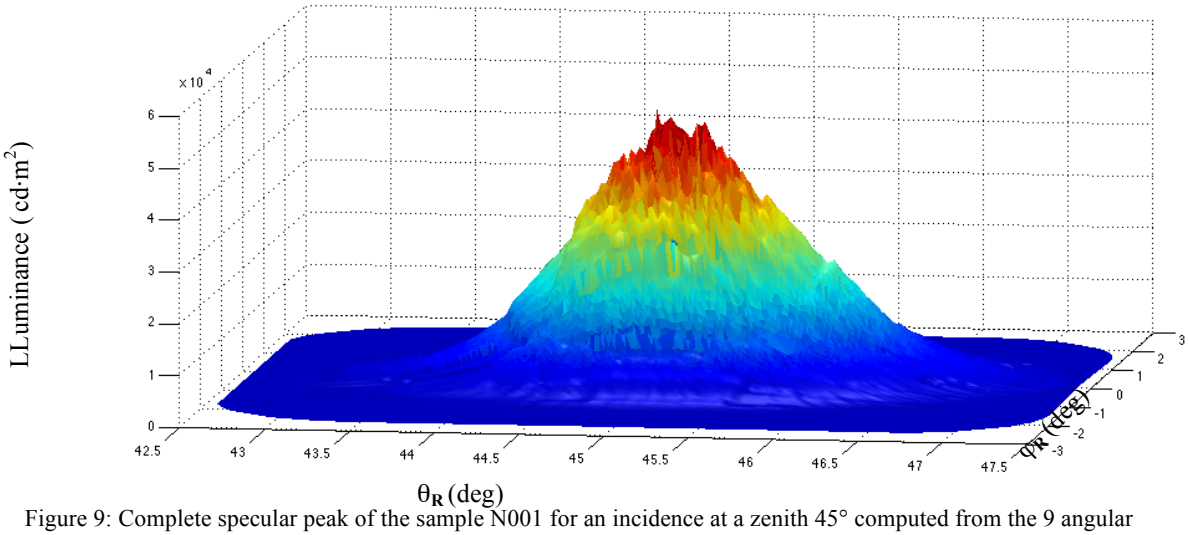


Figure 9: Complete specular peak of the sample N001 for an incidence at a zenith 45° computed from the 9 angular configuration, with 3 exposure times for each configuration (27 pictures in total). The angular resolution is 0,004° and the total number of direction measured is 1,4M. The luminance is plot in the vertical abscise.

We validated the system for a resolution of 0,03°, which is equal to the acuity of the "regular" visual system. We also validated the method that allows to compile different exposure times and adjacent pictures. Then, we have the possibility to scan more width peak with no limit of size, except maybe the number of data and the time of measurement and of data processing.

This device is young. We just finished the validation during 2013. In the future, we hope that it will provide new information on the specular peak of glossy materials. It could help to understand better the relation between roughness and BRDF and between BRDF and visual perception of gloss.

This facility will be used between 2014 and 2016 in the EMRP project xDReflect [17], to complete task in the workpackage 2, devoted to Gloss.

REFERENCES

1. CIE 175:2006, A framework for the measurement of visual appearance, International Commission on Illumination, (2006)
2. Zorll, U., "New aspects of gloss of paint film and its measurement", *Progress in Organic Coatings,* **1**, 113-155, 1972.
3. Christie, J., "Evaluation of the attribute of appearance called gloss", CIE-Journal, **5**, 2, 41-56, (1986).
4. International Standard ISO 2813, "Paint and varnishes – Measurement of the Specular Gloss of Non-metallic Paint Films at 20°, 60° and 85°", International Organization for Standardization, Geneva, (1978)
5. Obein, G., Knoblauch, K., . and Viénot, F., "Difference scaling of gloss: Nonlinearity, binocularity, and constancy", Journal of Vision **4**(9), 711-720 (2004)
6. Ji, W., Pointer, M., Luo, R., and Dakin, J., " Gloss as an aspect of the measurement of appearance," J. Opt. Soc. Am. A **23**, 22-33 (2006)
7. Doerschner, K., Boyaci, H., Maloney, L., « Estimating the glossiness transfer function induced by illumination change and testing its transitivity », *Journal of Vision*, **10**(4), 8. (2010).
8. Olkkonen, M., Brainard, D. « Perceived glossiness and lightness under real-world Illumination », *Journal of Vision*, **10**(9), 5 (2010).
9. Leloup, F., Pointer, M., Dutré, P., Hanselaer, P. « Geometry of illumination, luminance contrast, and gloss perception ». *J Opt Soc Am A*, 27, pp2046-2054. (2010)

10. Vienot, F. , Obein, G., “Is gloss recognized as a surface property?”, *Proceedings of MS 2004, 1st International Workshop on Materials and Sensations*, Pau, France, 27-29 October 2004, pages 77-82 (2004).
11. Ged, G., Obein, G., Silvestri, S., Le Rohellec, J., Viénot, F., “recognizing real materials from their glossy appearance”, *Journal of vision*, **10** (9),18 (2010).
12. Marlow, P., Anderson, B., “Generative constraints on image cues for perceived gloss”, *Journal of Vision*, **13**(14), 2, 1–23, (2013)
13. Obein, G. and Viénot, F., "Modelling the BRDF of a series of matt to glossy black samples", Proceedings of the CIE Expert Symposium on Visual Appearance, CIE publication x032:2007, 67-74 (2007)
14. Ouarets, S., Ged, G., Razet, A. and Obein, G., "A new gonioreflectometer for the measurement of the bidirectional reflectance distribution function (brdf) at LNE-CNAM", Proceedings of CIE 2012 "Lighting Quality and energy efficiency", 687-691 (2012)
15. Leroux, T., “Fast contrast vs viewing angle measurements of LCDs”, *Eurodisplay*, Strasbourg, 447 (1993)
16. Nicodemus, F., Richmond, J., Hsia, J., Ginsberg, I., Limperis T., “Geometrical considerations and nomenclature for reflectance”, US Dept. of Commerce, National Bureau of Standards., US Govt. Print. Off. (1977)
17. Visit www.xdreflect.eu

ACKNOWLEDMENT

This work has been partially funded by the Europeen Metrological Research Program (EMRP) carried on under the framework of the EURAMET agreement.